

SUPPORTING INFORMATION

Development of Selective Inhibitors for Aldehyde Dehydrogenases based on Substituted Indole-2,3-diones

Ann C. Kimble-Hill, Bibek Parajuli, Che-Hong Chen, Daria Mochly-Rosen, Thomas D. Hurley

Supplementary figures

Figure S1	S2
Figure S2	S2
Figure S3	S3
Figure S4	S3
Figure S5	S4
Figure S6	S4
Figure S7	S5
Figure S8	S5
Figure S9	S6
Figure S10	S6
Figure S11	S7
Figure S12	S7
Figure S13	S8
Figure S14	S8
Figure S15	S9
Figure S16	S9
Figure S17	S10
Figure S18	S10
Figure S19	S11
Figure S20	S11
Figure S21	S12
Figure S22	S12
Figure S23	S13
Figure S24	S13
Figure S25	S14
Figure S26	S14
Figure S27	S15
Figure S28	S15
Figure S29	S16
Figure S30	S16
Figure S31	S17
Figure S32	S17

Figure S1. Lineweaver-Burk plot of the non-linear fit to the non-competitive inhibition equation for the effect of **1** versus varied NAD^+ at fixed saturating propionaldehyde concentration on ALDH2. The plots shown are fits based on \bullet 0, \circ 2, \blacktriangledown 2.5, Δ 2.75, and \blacksquare 3 μM inhibitor concentrations.

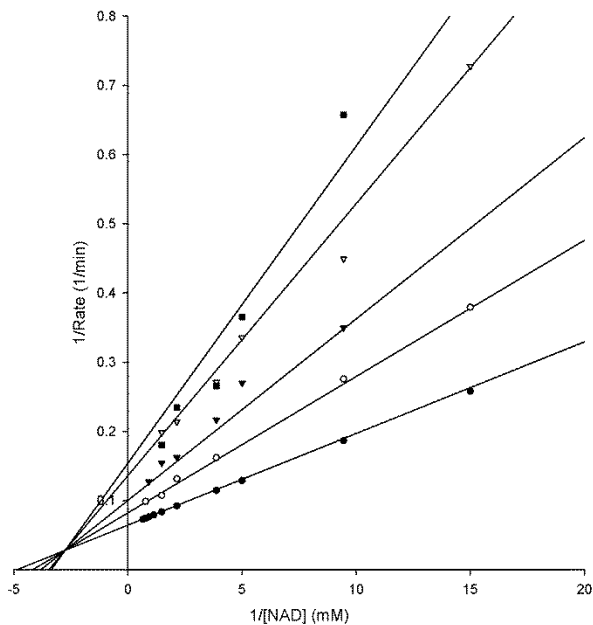


Figure S2. Lineweaver-Burk plot of the non-linear fit to the non-competitive inhibition equation for the effect of **3** versus varied NAD^+ at fixed saturating propionaldehyde concentration on ALDH2. The plots shown are fits based on \bullet 0, \circ 10, \blacktriangledown 25, Δ 50, and \blacksquare 70 μM inhibitor concentrations.

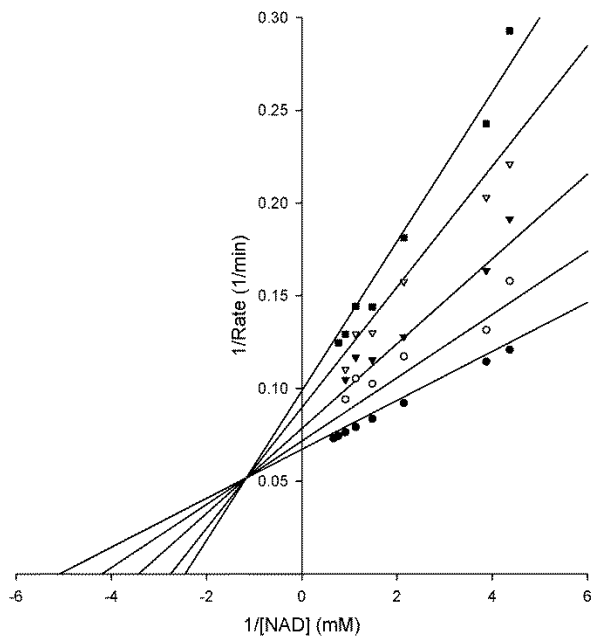


Figure S3. Lineweaver-Burk plot of the non-linear fit to the non-competitive inhibition equation for the effect of **1** versus varied NAD^+ at fixed saturating propionaldehyde concentration on ALDH1. The plots shown are fits based on \bullet 0; \circ 0.14, \blacktriangledown 0.28, Δ 0.57, and \blacksquare 0.71 μM inhibitor concentrations.

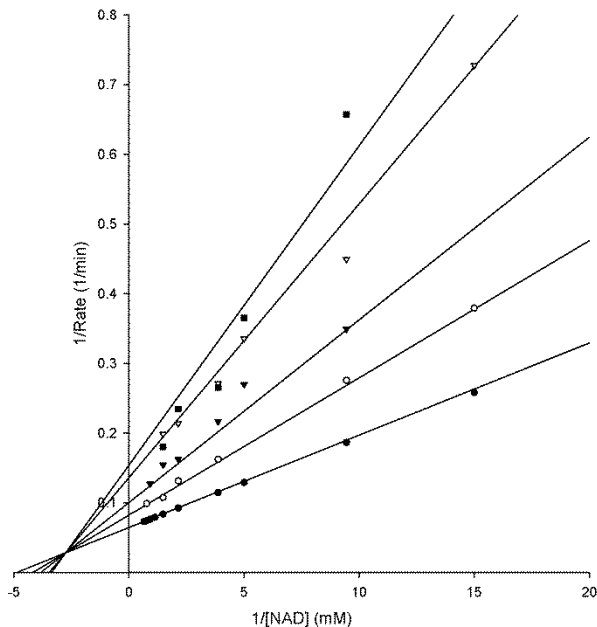


Figure S4. Lineweaver-Burk plot of the non-linear fit to the non-competitive inhibition equation for the effect of **1** versus varied NADP^+ at fixed saturating benzaldehyde concentration on ALDH3. The plots shown are fits based on \bullet 0; \circ 0.15, \blacktriangledown 0.20, Δ 0.45, \blacksquare 0.62, and \square 0.99 μM inhibitor concentrations.

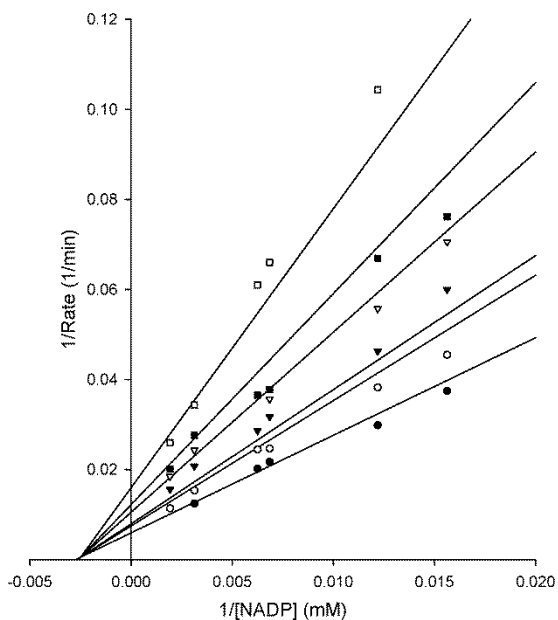


Figure S5. Lineweaver-Burk plot of the non-linear fit to the non-competitive inhibition equation for the effect of **3** versus varied NADP^+ at fixed saturating benzaldehyde concentration on ALDH3. The plots shown are fits based on \bullet 0, \circ 3, \blacktriangledown 5, Δ 8, \blacksquare 10, and \square 25 μM inhibitor concentrations.

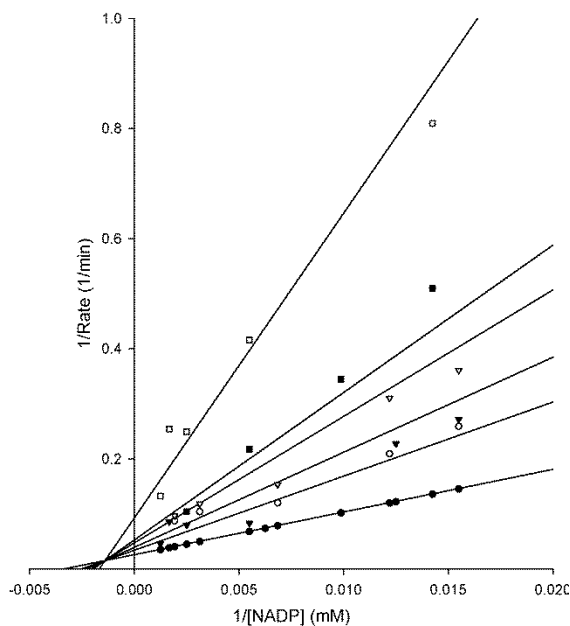


Figure S6. Lineweaver-Burk plot of the non-linear fit to the non-competitive inhibition equation for the effect of **1** versus varied propionaldehyde at fixed saturating NAD^+ concentration on ALDH2. The plots shown are fits based on \bullet 0, \circ 0.33, \blacktriangledown 0.67, Δ 1, \blacksquare 2, and \square 3.3 μM inhibitor concentrations.

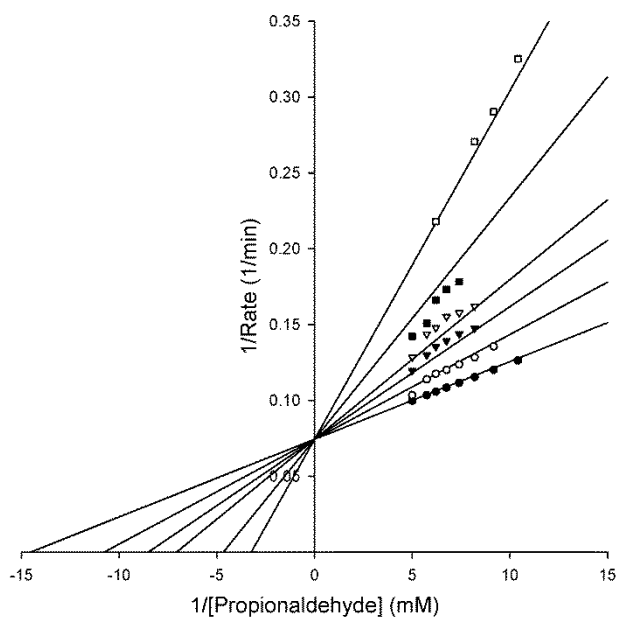


Figure S7. Lineweaver-Burk plot of the non-linear fit to the non-competitive inhibition equation for the effect of **3** versus varied propionaldehyde at fixed saturating NAD^+ concentration on ALDH2. The plots shown are fits based on \bullet 0, \circ 50, \blacktriangledown 70, and Δ 150 μM inhibitor concentrations.

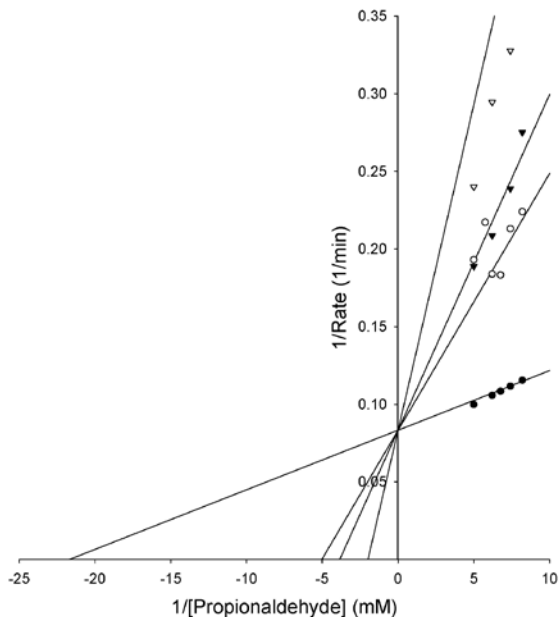


Figure S8. Lineweaver-Burk plot of the non-linear fit to the non-competitive inhibition equation for the effect of **1** versus varied propionaldehyde at fixed saturating NAD^+ concentration on ALDH1. The plots shown are fits based on \bullet 0, 0.36, \blacktriangledown 0.48, and Δ 0.8 μM inhibitor concentrations.

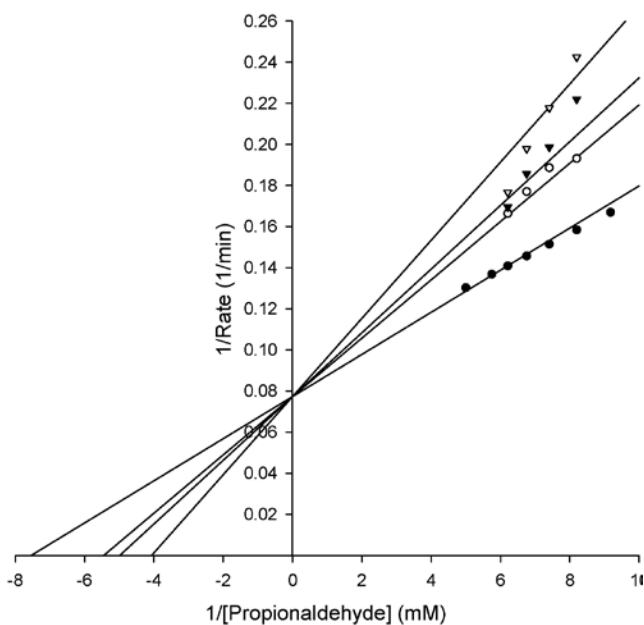


Figure S9. Lineweaver-Burk plot of the non-linear fit to the non-competitive inhibition equation for the effect of **1** versus varied benzaldehyde at fixed saturating NADP⁺ concentration on ALDH3. The plots shown are fits based on • 0, ◊ 0.19, ▼ 0.49, and Δ 0.79 μM inhibitor concentrations.

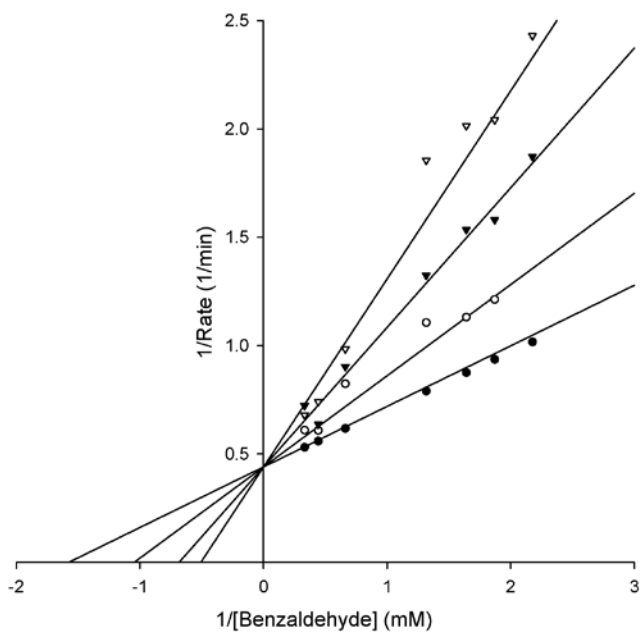


Figure S10. Lineweaver-Burk plot of the non-linear fit to the non-competitive inhibition equation for the effect of **3** versus varied benzaldehyde at fixed saturating NADP⁺ concentration on ALDH3. The plots shown are fits based on • 0, ◊ 1, ▼ 2.5, Δ 5, and ■ 7 μM inhibitor concentrations.

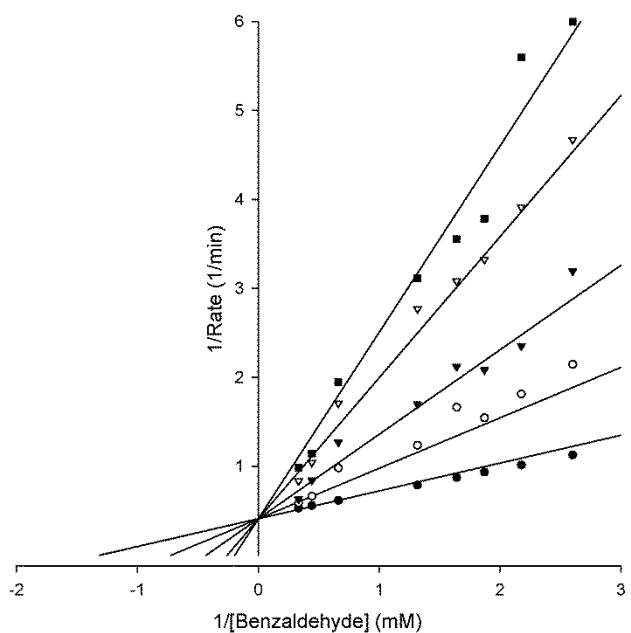


Figure S11. NMR Spectra provided by vendor of 1-benzyl-5-bromo-1H-indole-2,3-dione (5).

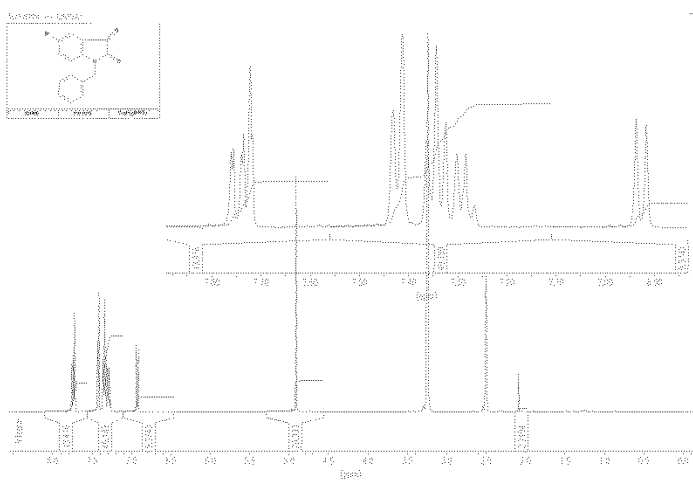


Figure S12. NMR Spectra provided by vendor of 1-(2-phenylethyl)-1H-indole-2,3-dione (6).

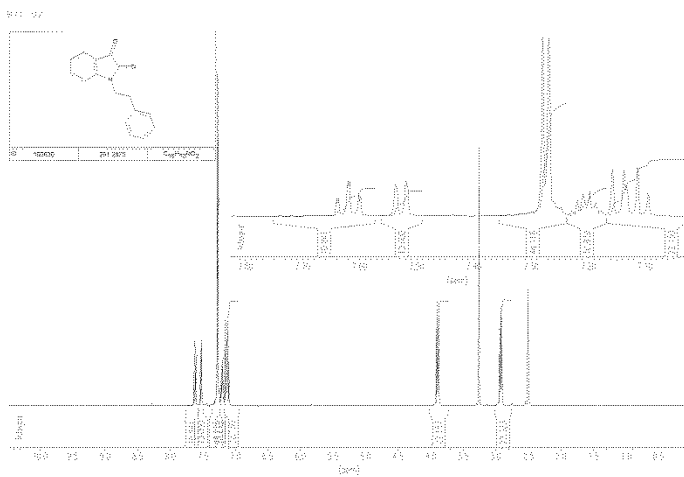


Figure S13. NMR Spectra provided by vendor of 5-chloro-1-(2-phenylethyl)-1H-indole-2,3-dione (**7**).

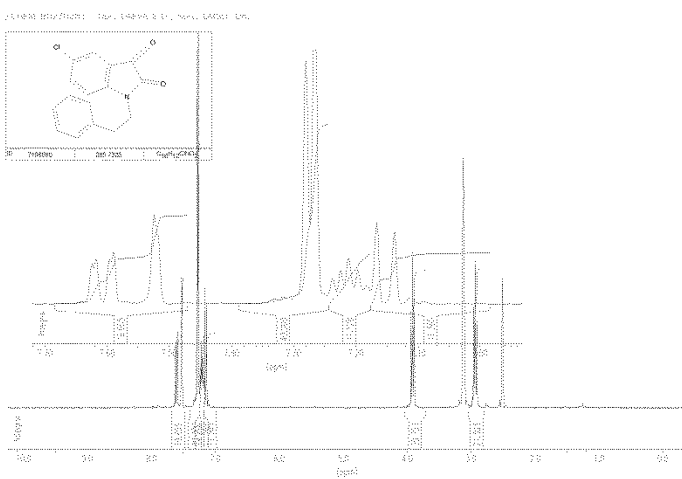


Figure S14. NMR Spectra provided by vendor of 5-bromo-1-(2-phenylethyl)-1H-indole-2,3-dione (**8**).

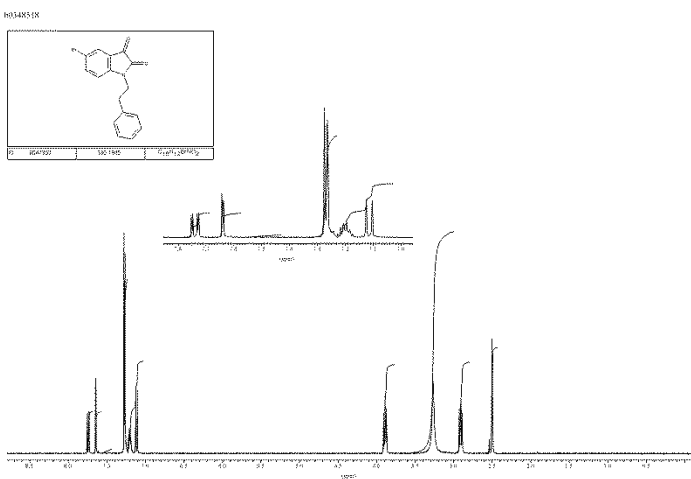


Figure S15. NMR Spectra provided by vendor of 7-bromo-5-methyl-1H-indole-2,3-dione (**1**).

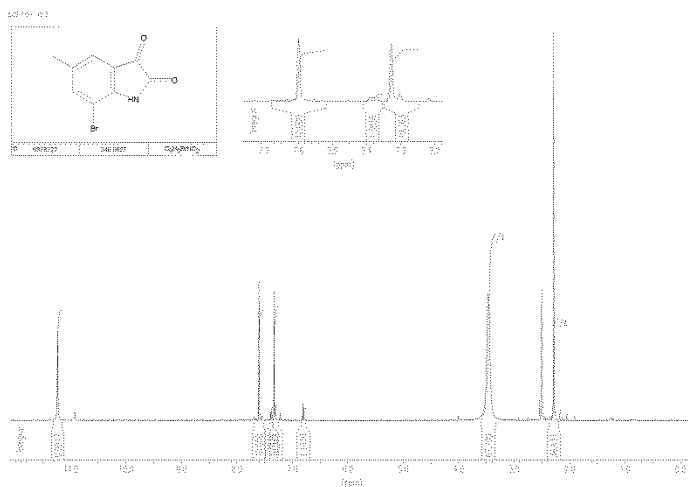


Figure S16. NMR Spectra provided by vendor of 1-(3-phenylpropyl)-1H-indole-2,3-dione (**9**).

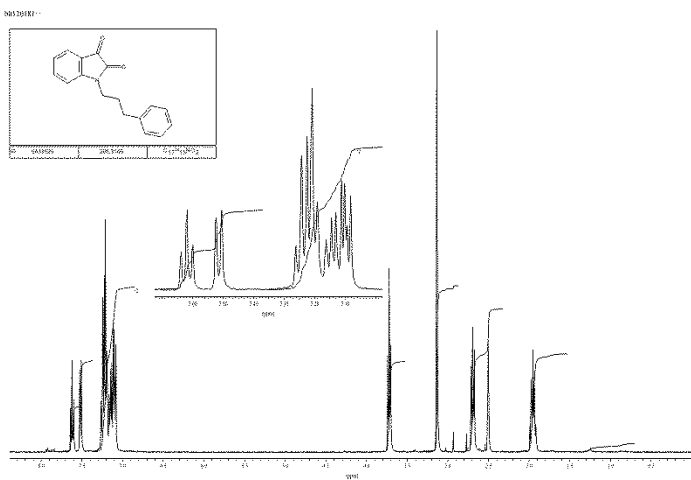


Figure S17. NMR Spectra provided by vendor of 1-(3-phenyl-2-propen-1-yl)-1H-indole-2,3-dione (**10**).

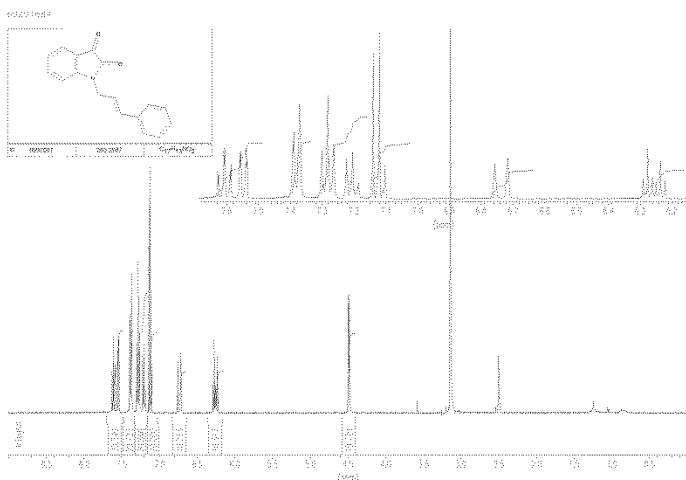


Figure S18. NMR Spectra provided by vendor of 1-{[4-(1,3-benzodioxol-5-ylmethyl)-1-piperazinyl]methyl}-1H-indole-2,3-dione (**20**).

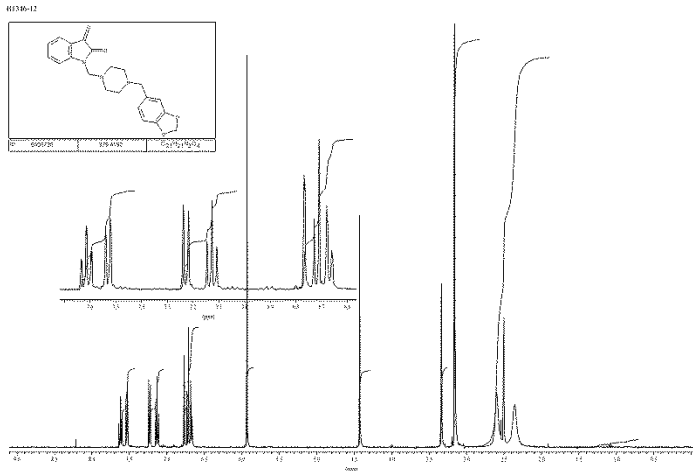


Figure S19. NMR Spectra provided by vendor of 1-{[4-(4-fluorobenzyl)-1-piperazinyl]methyl}-1H-indole-2,3-dione (**16**)

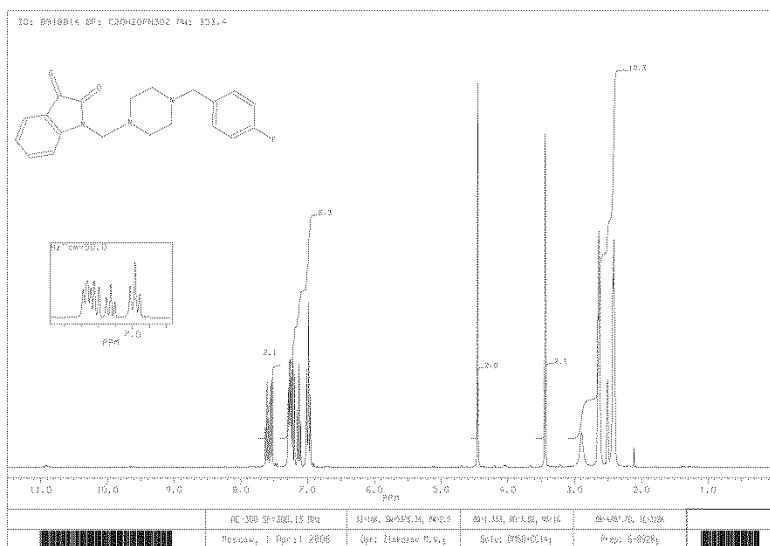


Figure S20. NMR Spectra provided by vendor of 1-{[4-(3-chlorobenzyl)-1-piperazinyl]methyl}-1H-indole-2,3-dione (**18**).

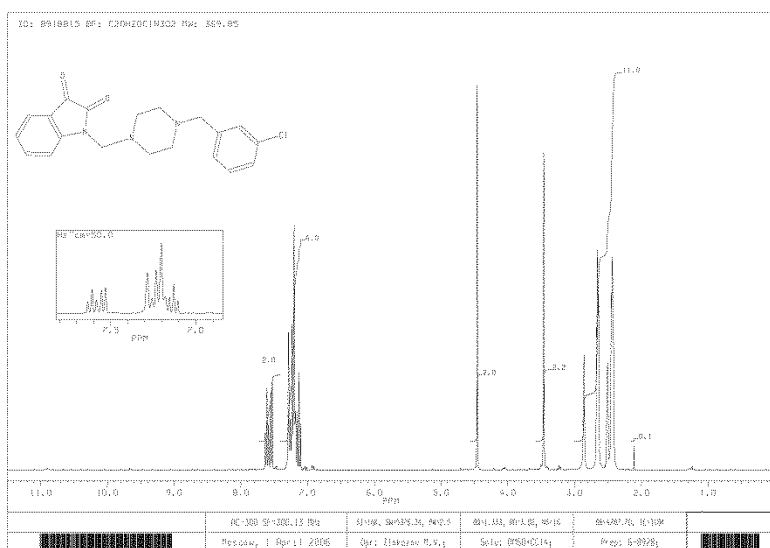


Figure S21. NMR Spectra provided by vendor of 1-{[4-(2-fluorobenzyl)-1-piperazinyl]methyl}-1H-indole-2,3-dione (**15**).

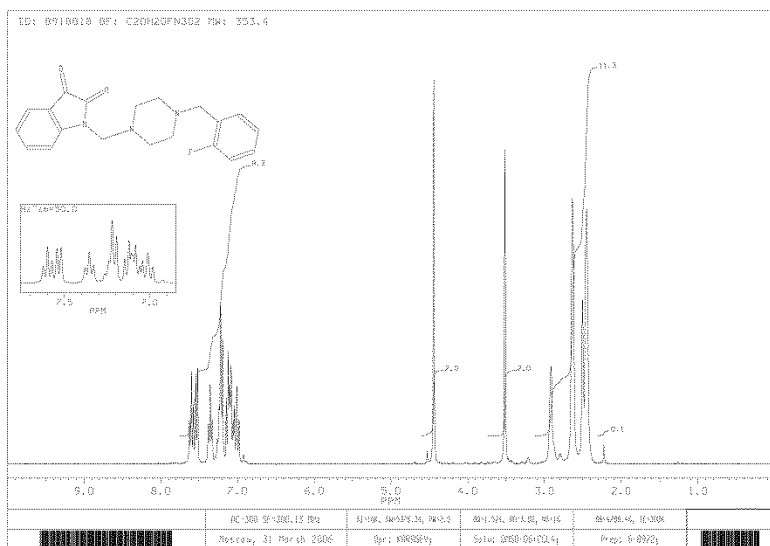


Figure S22. NMR Spectra provided by vendor of 1-{[4-(3-fluorobenzyl)-1-piperazinyl]methyl}-1H-indole-2,3-dione (**17**).

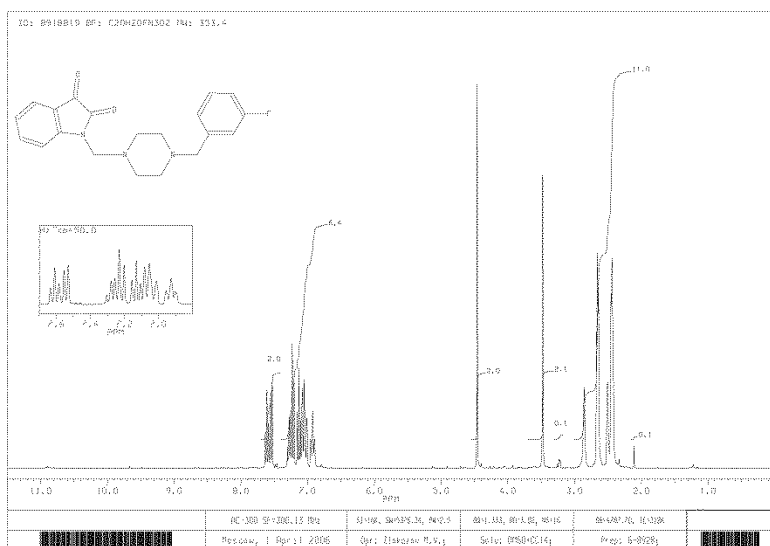


Figure S23. NMR Spectra provided by vendor of 1-[4-(3-methoxybenzyl)-1-piperazinyl]methyl]-1H-indole-2,3-dione (**19**).

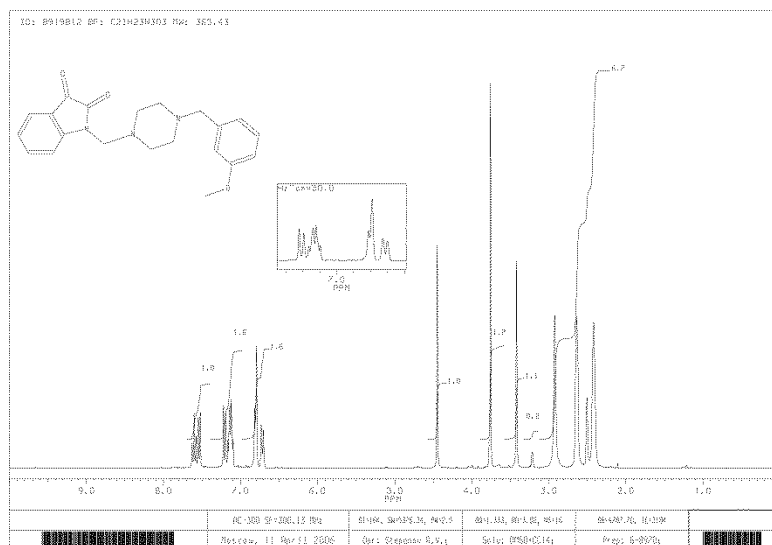


Figure S24. NMR Spectra provided by vendor of 1-[4-(1,3-benzodioxol-5-ylmethyl)-1-piperazinyl]methyl]-5-bromo-1H-indole-2,3-dione (**21**).

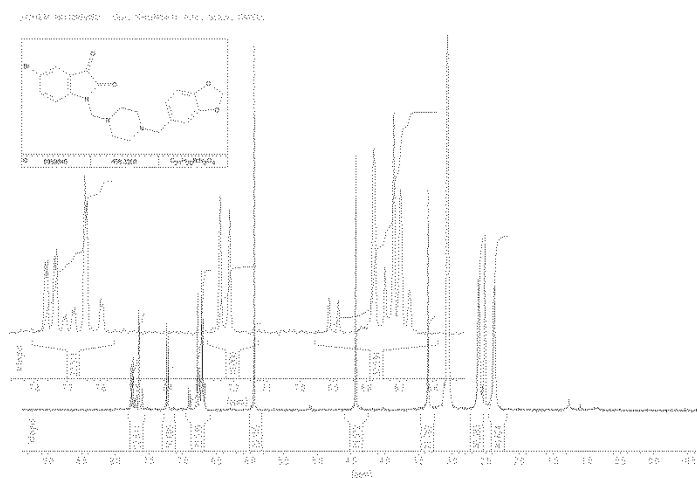


Figure S25. NMR Spectra provided by vendor of 1,1'-[1,3-imidazolidinediylbis(methylene)]bis(1H-indole-2,3-dione) (**22**).

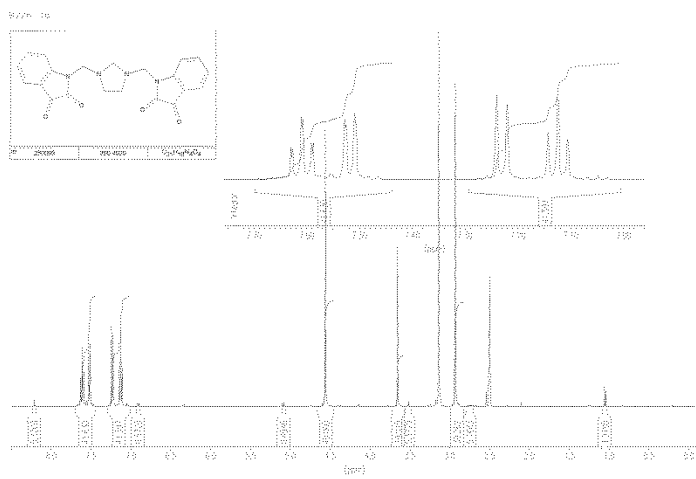


Figure S26. NMR Spectra provided by vendor of 1-(4-morpholinylmethyl)-1H-indole-2,3-dione (**12**).

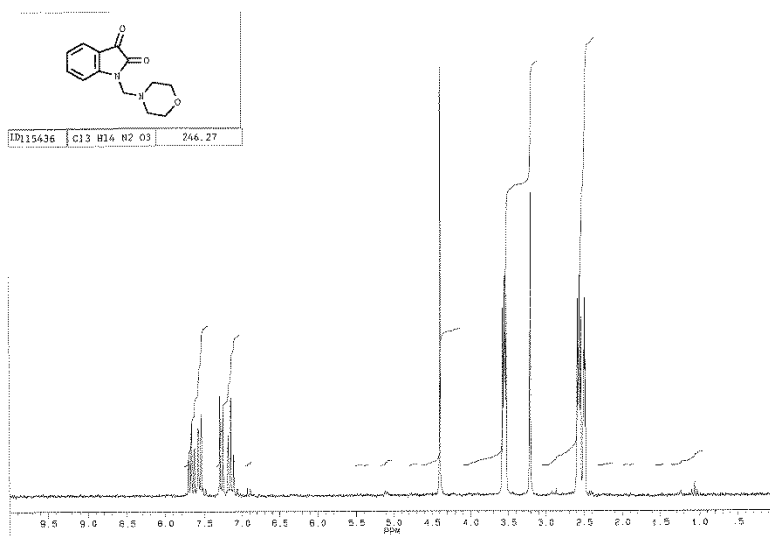


Figure S27. NMR Spectra provided by vendor of 1-[(4-methyl-1-piperazinyl)methyl]-1H-indole-2,3-dione (**13**).

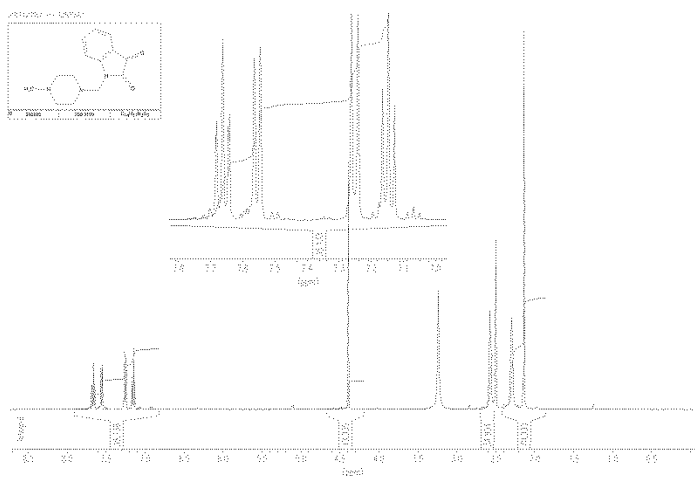


Figure S28. NMR Spectra provided by vendor of 1-[(4-benzyl-1-piperazinyl)methyl]-1H-indole-2,3-dione (**14**).

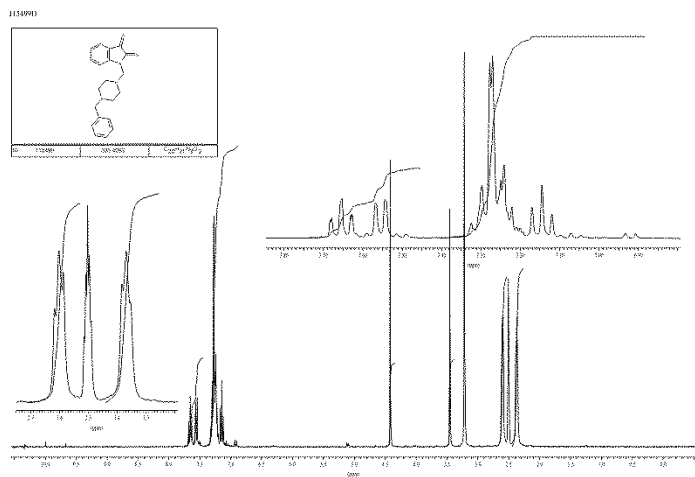


Figure S29. NMR Spectra provided by vendor of 1-pentyl-2,3-dihydro-1H-indole-2,3-dione (2).

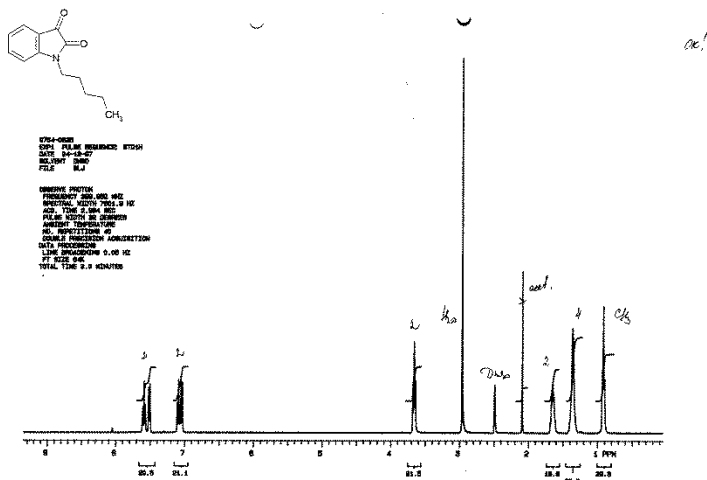


Figure S30. NMR Spectra provided by vendor of 1-benzyl-2,3-dihydro-1H-indole-2,3-dione (3).

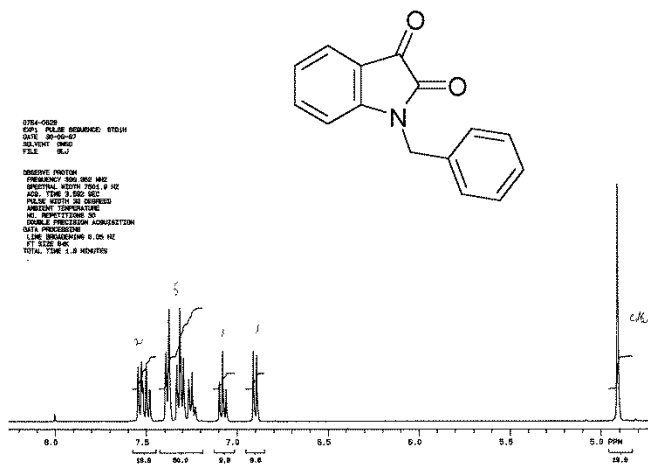


Figure S31. NMR Spectra provided by vendor of 1-benzyl-5-chloro-2,3-dihydro-1H-indole-2,3-dione (**4**) (PO # 950549)

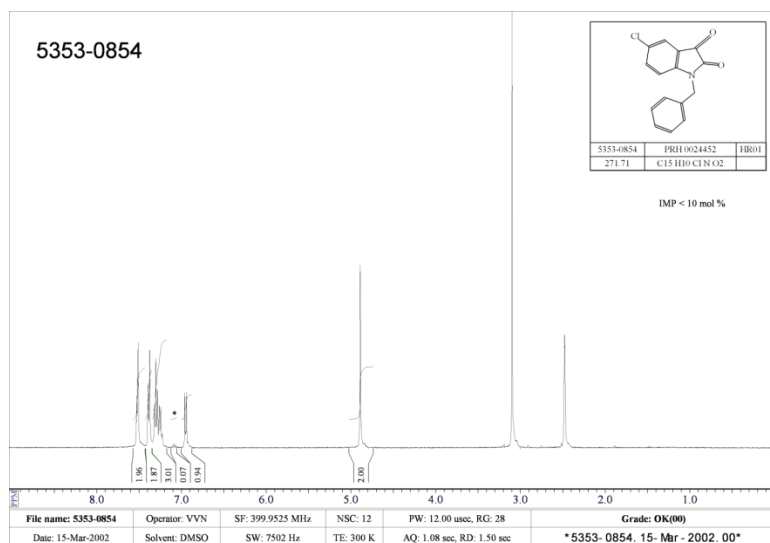


Figure S32. NMR Spectra provided by vendor of 5-chloro-1-[(2E)-3-phenylprop-2-en-1-yl]-2,3-dihydro-1H-indole-2,3-dione (**11**)

